

## High- $\beta$ Plasmoid Drift during Pellet Injection into Tokamaks

H.W. Müller, K. Büchl, M. Kaufmann, P.T. Lang, R.S. Lang, A. Lorenz,  
V. Mertens, J. Neuhauser and ASDEX Upgrade Team

MPI für Plasmaphysik, EURATOM-Association, D-85748 Garching, Germany

**Introduction** When a frozen hydrogen isotope pellet is injected into a hot, magnetically confined plasma, pellet material is quickly ablated, ionized and heated (mostly) by fast electron energy influx along magnetic field lines [1]. Since the expansion of the ablation cloud parallel to the magnetic field is much slower, the energy density in the ablation cloud is rapidly increased over the ambient plasma pressure, and a localised high- $\beta$  plasmoid is formed. In an inhomogeneous magnetic field as in toroidal magnetic traps, this high- $\beta$  plasmoid tends to be expelled from the magnetic field [1,2,3]. For an axisymmetric tokamak geometry the diamagnetic plasmoid should be quickly accelerated in major radius direction, favouring clearly pellet launch from the magnetic high field side (HFS) over standard low field side (LFS) injection, as confirmed recently in ASDEX Upgrade [4]. In the present paper we report on the direct observations of the predicted drift, analyse the plasmoid dynamics and compare with model predictions. First results about the plasmoid heating are shown. The high- $\beta$  plasmoid drift seems also to affect the pellet motion in the plasma leading to an acceleration of the pellet in direction of the drift.

**Experimental Arrangement** The pellets at ASDEX Upgrade are accelerated by means of a centrifuge. A funnel is used to feed them into a guiding tube for HFS pellet injection,

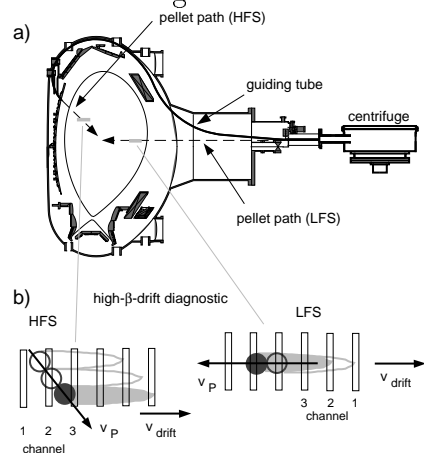


**Figure 1:** a) Cross section of ASDEX Upgrade. The pellet injection is performed by means of a centrifuge via guiding tubes. The high- $\beta$ -drift observation system is looking toroidally at the high- $\beta$  plasmoid drift. b) At the HFS and LFS the drift is observed by 10 lines of sight.

3 – 4 mm and its height about 30 mm. Figure 1b) shows the motion of the pellet and the drifting plasmoids relative to the diagnostic channels. The intensity at two preselected wavelengths can be measured simultaneously for each line of sight. This allows to

where the pellets are injected under  $44^\circ$  to the horizontal plane (figure 1a)) [4]. For LFS injection the guiding tube can be moved vertically and the pellets fly freely, horizontally into the plasma close to the midplane. This injection scheme limits the pellet velocity to  $v_P = 240 \text{ ms}^{-1}$ . In the experiments described here Deuterium (D) pellets are injected with a repetition rate of 30 – 60 Hz and a particle content of  $2.7 - 3.8 \times 10^{20}$  atoms into D plasmas. The plasma current is 800 kA, the magnetic field at the plasma axis is 1.8 – 2.1 T the safety factor is  $q_{95} = 3.9 - 4.2$  and the plasma elongation  $\kappa = 1.6$ .

In order to observe the high- $\beta$  plasmoid drift dynamics in detail a new diagnostic system with high space and time resolution has been installed in the ASDEX Upgrade vacuum chamber viewing toroidally at the pellet path. For both LFS and HFS pellet injection there is one array with 10 lines of sight each. The spatial distance of two neighbouring channels is about 15 mm. The width of each observation channel is

determine the temperature of the plasmoid. The continuum radiation at 538.1 nm and the D $_{\alpha}$ -line emission are used for the high- $\beta$ -drift observation. The signals are monitored with a temporal resolution of 1  $\mu$ s. Alternatively, the density can be obtained from Stark broadening by means of a spectrometer.

**High- $\beta$ -Drift Dynamics** Figure 2a) shows typical signals of two channels in the case of LFS pellet injection (line averaged electron density  $\bar{n}_e = 5.4 \times 10^{19} \text{ m}^{-3}$ , heating power of neutral beam injection  $P_{NI} = 2.5 \text{ MW}$ , electron temperature in the plasma centre  $T_{e,0} \sim 1500 \text{ eV}$ , ion temperature  $T_{i,0} \sim 1500 \text{ eV}$ ). Channel 4 shows a broad peak first, followed by a sequence of distinct spikes with decreasing intensity. The same signature is seen in channel 5 with a temporal shift of 73  $\mu$ s corresponding to a velocity of 225  $\text{ms}^{-1}$ . This is slightly less than the nominal pellet velocity. The last spikes are monitored 200  $\mu$ s after the onset of the signal sequence while the ablation cloud needs only  $\approx 60 \mu$ s to

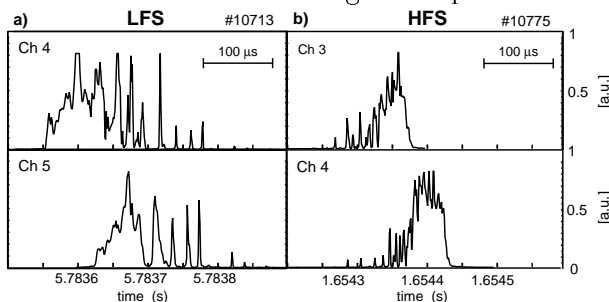


**Figure 2:** Signals detected by the new observation system in the case of a) LFS and b) HFS pellet injection. The time traces show continuum radiation. A higher channel number indicates a line of sight closer to the plasma centre.

channels. This is much higher than the nominal speed of  $v_P = 175 \text{ ms}^{-1}$  in this direction.

The observed sequences for LFS and HFS pellet injection are, in fact, what has to be expected for the occurrence of a fast acceleration to the torus outside up to velocities far exceeding  $v_P$ . For LFS pellet injection a channel of the observation system will first monitor the emission of the ablation cloud passing the line of sight, a strong signal of the slowly moving ablation cloud. When the pellet with its ablation cloud left the line of sight, plasmoids moving backwards to the torus outside cross the channel (figure 1b)). The signal decrease is caused by the expansion and heating of the plasmoids which reduce both, D $_{\alpha}$ -line emission and continuum radiation. In the case of HFS pellet injection the first plasmoids created closer to the plasma edge reach a specific line of sight. The first plasmoids reaching the channel travel over the longest distance causing the lowest radiation intensity. The intensity is increasing until the broad, strong maximum is reached when the ablation cloud passes the channel. After the ablation cloud left the line of sight, the signal ends abruptly.

The separation into discrete spikes is related to the formation of striations. In figure 3a) the signal of a diode observing the whole pellet ablation is shown. The oscillations seen in this signal are corresponding to the well known striations occurring during the pellet ablation [5]. While the pellet with its ablation cloud crosses one line of sight of the high- $\beta$ -drift diagnostic, this oscillation is also seen locally (grey underlayed region in figure 3). It is caused by density fluctuations while the temperature stays constant. The density oscillation leads to a separation of the ablated material into discrete plasmoids. The high-

cross the line of sight. The spike duration is down to 1  $\mu$ s. The sequence of observation is inverted in the case of HFS pellet injection as shown in figure 2b) ( $\bar{n}_e = 9.4 \times 10^{19} \text{ m}^{-3}$ ,  $P_{NI} = 4.9 \text{ MW}$ ,  $T_{e,0} \sim 1700 \text{ eV}$ ). Here the separated spikes with an increasing intensity are monitored first and the sequence ends with a strong, broad peak. A velocity of about 300  $\text{ms}^{-1}$  in major radius direction is determined from the end of the broad peaks of the diagnostic

$\beta$ -drift causes a temporal variation of the plasma shielding of the pellet and therefore the formation of striations as assumed in [6, 7]. In the case of HFS pellet injection channels

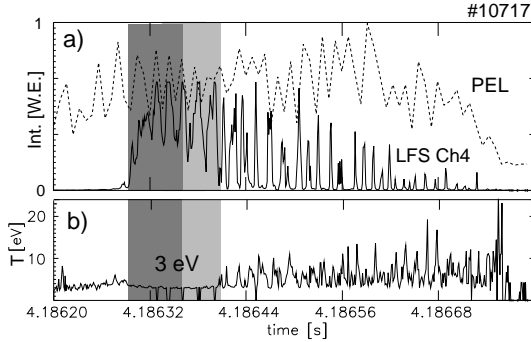


**Figure 3:** a) Comparison of the D $\alpha$  emission detected by a diode observing the whole pellet ablation (broken line) and the time trace of one channel of the new diagnostic,  $\lambda = 538.1$  nm (solid line). b) Temperature determined from the ratio of line to continuum emission. The grey boxes indicate the minimum and maximum time the pellet will need to cross the line of sight.

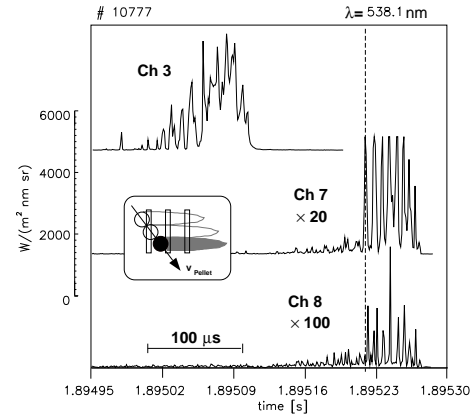


**Figure 4:** Time traces of 3 diagnostic channels during HFS pellet injection. Channel 7 and 8 closer to the plasma centre than channel 3 monitor drifting plasmoids only. The signal of channel 7 is enhanced by a factor of 20, channel 8 by a factor of 100. The largest peaks of channel 7 are in saturation.

closer to the plasma centre detect only radiation emitted by plasmoids drifting to the torus outside. This is shown in figure 4. The plasma parameters are  $\bar{n}_e = 7.2 \times 10^{19} \text{ m}^{-3}$ ,  $P_{NI} = 4.9 \text{ MW}$ ,  $T_{e,0} \sim 2200 \text{ eV}$  and  $T_{i,0} \sim 2000 \text{ eV}$ . Channel 3 shows the typical behaviour in the case of HFS injection as seen before. But channel 7 and 8 show only a strongly oscillating signal without a broad peak. Here the pellet penetrates only up to channel 6 into the plasma. Therefore the signals in the channels 7 and 8 must be caused by a drift to the magnetic LFS.

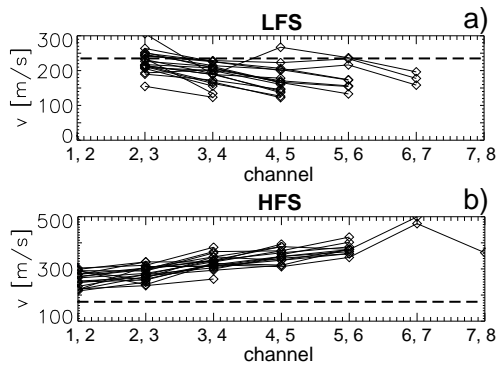
The time delay between the channels 7 and 8 of  $1 - 3 \mu\text{s}$  corresponds to a drift velocity  $v_D = 5 \times 10^3 - 1.6 \times 10^4 \text{ ms}^{-1}$ . The peaks can be followed up over several channels, sometimes even over 5 or 6 channels is possible, shows drift velocities of  $10^3 - 10^4 \text{ ms}^{-1}$  and an acceleration of  $10^8 - 10^9 \text{ ms}^{-2}$ . Theoretically an acceleration of  $a_D^{theo} = 4\gamma k_B T_{e,pl} / (m R_{pl} \sim 10^9 \text{ ms}^{-2})$  was expected [8] ( $\gamma$  is the adiabaticity coefficient,  $k_B T_{e,pl}$  the electron energy inside the plasmoid,  $m$  the ion mass and  $R_{pl}$  the major radius). A new equilibrium will establish on the shear Alfvén transit time over a connection length  $\sim 5 \mu\text{s}$  [4]. Together with  $a_D^{theo}$  a drift velocity of  $10^3 - 10^4 \text{ ms}^{-1}$  was expected. There is a good agreement of the expected and measured acceleration and drift velocity.

**Plasmoid temperature and density** From the ratio of D $\alpha$ -line to continuum emission the plasmoid temperature can be calculated. Inside the ablation cloud temperatures of  $3 - 6 \text{ eV}$  have been measured (figure 3b)) which agrees with measurements at other tokamaks [5]. The first plasmoids have temperatures of about  $\sim 5 \text{ eV}$  in the centre, at the edge the temperatures seem to reach  $\sim 10 \text{ eV}$ . For the pellet shown in figure 4, the temperature obtained from the signals of channel 8 ( $5 - 10 \mu\text{s}$  after ablation) is  $\approx 20 - 30 \text{ eV}$ .

The plasmoid densities are determined from Stark broadening of the D $\alpha$ -line. During the pellet ablation typically densities of  $10^{23} - 10^{24} \text{ m}^{-3}$  are found like in other experiments

[5]. Therefore the plasmoid beta  $\beta_{pl} = 2\mu_0 p_{pl}/B^2$  ( $p_{pl}$  is the kinetic pressure inside the plasmoid,  $B$  the magnetic field strength) is during the ablation process typically enhanced by a factor of 30 compared to  $\beta_0$  of the background plasma. After the separation of plasmoid and pellet  $\beta_{pl}$  will first raise by a factor of 2 – 5, before decreasing.

**Pellet Acceleration** A pellet injected from the LFS is decelerated while moving into the plasma (see lines in figure 5a) while in the case of HFS injection the radial directed velocity component increases (figure 5b)).



The guiding tube does not affect the pellet velocity in any way. On average the pellets are accelerated by several  $10^5 \text{ ms}^{-1}$ . The acceleration is in both cases directed to the torus outside. A frictional momentum transfer or a net rocket effect caused by the high- $\beta$ -drift are the most probably processes to cause this acceleration.

**Figure 5:** Pellet velocities between two diagnostic channels for LFS and HFS pellet injection. The broken lines indicate the nominal radial pellet velocity.

**Summary and Conclusions** At ASDEX Upgrade the high- $\beta$  plasmoid drift has been observed for the first time during LFS and HFS pellet injection. Immediately after ablation discrete high- $\beta$  plasmoids drift to the magnetic LFS, independently of the direction of pellet motion. The measured acceleration of  $10^8 - 10^9 \text{ ms}^{-2}$  and drift velocities of  $10^3 - 10^4 \text{ ms}^{-1}$  are consistent with the theoretically expected values, and have been observed similarly for LFS pellet injection at the RTP tokamak [7]. While the ablation cloud passes one line of sight of a diagnostic the temperature stays constant and the density is oscillating. This causes the formation of striations during the ablation process and a sequence of discrete, drifting plasmoids develops. These plasmoids are strongly heated (several 10 eV in 5 – 10  $\mu\text{s}$ ) and  $\beta_{pl}$  is still raising during the first  $\mu\text{s}$  of the drift. The drift causes an acceleration of the pellet to the torus outside.

The high- $\beta$ -drift has a strong effect on the ablation dynamics due to the removal of the plasma shielding [1]. It causes a strong particle loss in the case of LFS pellet injection. In hot plasmas at ASDEX Upgrade the fueling efficiency is reduced to 30 % [4]. For HFS pellet injection the high- $\beta$  plasmoid drift moves the ablated material to the plasma centre. Therefore the fueling efficiency is not reduced and the material is deposited closer to the plasma centre. The high- $\beta$ -drift clearly favours pellet injection from the magnetic HFS for hot plasmas and will support central plasma fueling of big fusion devices.

## references

- [1] M. Kaufmann, K. Lackner, L. Lengyel, and W. Schneider, Nucl. Fusion **27**, 1986.
- [2] V.A. Rozhansky et al., Plasma Phys. and Contr. Fusion **37**, 1995.
- [3] H.R. Strauss and W. Park, Phys. Plasmas **5**, 1998.
- [4] P.T. Lang et al., Phys. Rev. Lett. **79**, 1997.
- [5] S.L. Milora, W.A. Houlberg, L.L. Lengyel and V. Mertens, Nucl. Fusion **35**, 1995.
- [6] J. Neuhauser and R. Wunderlich, IPP Report, 5/30, 1989.
- [7] J. de Kloe et al., Phys. Rev. Lett. **82**, 1999.
- [8] L.L. Lengyel, Nucl. Fusion **17**, 1977.